Original Article
Received: 21-Mar-2008
Accepted: 28-Jul-2008

TRP-ML1 Functions as a Lysosomal NAADP-Sensitive Ca^{2+} Release Channel in Coronary Arterial Myocytes

Fan Zhang, Si Jin, Fan Yi and Pin-Lan Li

Department of Pharmacology & Toxicology,

Medical College of Virginia Campus,

Virginia Commonwealth University, VA 23298

Running title: TRP-ML1 Function as Lysosomal Ca^{2+} Release Channels

Send Correspondence and Reprint Requests to:

Pin-Lan Li, MD, Ph.D
Department of Pharmacology and Toxicology
Medical College of Virginia
Virginia Commonwealth University
410 North 12th Street
P.O. Box 980613
Phone: (804) 828-4793
Fax: (804) 828-4794
E-mail: **pli@vcu.edu**

This is an Accepted Work that has been peer-reviewed and approved for publication in the *Journal of Cellular and Molecular Medicine*, but has yet to undergo copy-editing and proof correction. See http://www.blackwell-synergy.com/loi/jcmm for details.
Please cite this article as a "Postprint";10.1111/j.1582-4934.2008.00486.x

ABSTRACT

Nicotinic acid adenine dinucleotide phosphate (NAADP) is a potent intracellular Ca^{2+} signaling second messenger, but the mechanism of NAADP-induced Ca^{2+} release is still poorly understood. The present study tested the hypothesis that NAADP induces Ca^{2+} release from the lysosomal store via a TRP-ML1 (transient receptor potential-mucolipin 1)-mediated Ca^{2+} release channel in coronary arterial myocytes (CAMs). RT-PCR and Western blot analyses demonstrated that TRP-ML1 was present in CAMs, and fluorescence resonance energy transfer (FRET) detection revealed that the TRP-ML1 was closely associated with some lysosomal proteins in these CAMs. ET-1, a well-known NAADP stimulator, was found to induce a local Ca^{2+} burst from lysosomes followed by a global Ca^{2+} release. This lysosome-associated Ca^{2+} release was significantly inhibited in the TRP-ML1 siRNA pre-treated CAMs by 46.8 ± 12.6 % in the local Ca^{2+} burst and 73.3 ± 14.9 % in the global Ca^{2+} wave. In the reconstituted lysosomal channels from CAMs, NAADP activated Ca^{2+} release channels at concentrations of 1-1000 nM, but neither activators (1 μM IP_3, 5 μM Rya) nor blockers (100 μM 2-APB, 50 μM Rya) of sarcoplasmic reticulum (SR) Ca^{2+} release channels had effect on the channel activity. Moreover, TRP-ML1 gene silencing reduced this NAADP-sensitive Ca^{2+} release channel activity in lysosomes by 71.5 ± 18.5%. Immunoprecipitation or blockade of TRP-ML1 by anti-TRP-ML1 antibodies almost abolished NAADP-induced activation of lysosomal Ca^{2+} channels (to 14.0 ± 4.4% of control). These results for the first time provide direct evidence that an NAADP-sensitive Ca^{2+} release channel is characteristic of TRP-ML1 channels.

Key Words: Transient receptor potential channel, lysosomal Ca^{2+} store, Ca^{2+} mobilization, organelles, coronary circulation

INTRODUCTION

Nicotinic acid adenine dinucleotide phosphate (NAADP) is a newly discovered intracellular Ca^{2+} signaling messenger in a wide variety of cells, from plants to animals including humans[1]. This NAADP-mediated Ca^{2+} release response may produce important physiological action or regulation[2]. It had been proposed that ADP-ribosyl cyclase (CD38) is the major enzyme involved in the NAADP formation with the base-exchange reaction in some mammalian tissues, in which the nicotinamide residue from NADP is replaced by nicotinic acid[3]. However, the physiological pathway for the synthesis of NAADP has yet to be defined to date, and the information regarding how this NAADP signaling neucleotide reaches its target Ca^{2+} store and interacts with the Ca^{2+} release channel are limited. Regarding the NAADP signal system, controversy exists over the identity of NAADP-related Ca^{2+} stores and the characterization of NAADP-sensitive Ca^{2+} release channels. Two working models have been proposed to interpret the different actions of NAADP in mobilizing intracellular Ca^{2+} release[4]. In the first model, the ER or SR that expresses IP_3Rs and RyRs is responsible for NAADP-induced Ca^{2+} release, in which NAADP may interact either directly with RyRs or via a separate protein that may indirectly activate RyRs[5, 6]. This model could be explained by several cell types such as T-lymphocytes, cardiac cells and skeletal muscle. The second model is related to a two-pool mechanism, which suggests that an NAADP-sensitive Ca^{2+} store is a thapsigargin-insensitive lysosome-like acidic store. This NAADP-sensitive Ca^{2+} store is responsible for a localized signal, which triggers Ca^{2+}-induced Ca^{2+} release (CICR) to cause global Ca^{2+} increases through IP_3Rs and RyRs on the SR[7-9]. This model works well on an increasing number of cell types such as sea urchin eggs, smooth muscle cells, pancreatic cells and hepatocytes.

Lysosomes are membrane-bound organelles, which originate from the Golgi apparatus and exist in the cytoplasm of all eukaryotic cells. Beyond intracellular digestion for cell defense, autophagy, and fertilization, recent studies have extended lysosomal function to cellular signaling in different cells[7-10]. On the lysosomal membrane, there is an H^+-ATPase that functions to acidify the vesicle compartmental environment and then facilitate the activity of various acid hydrolases. Furthermore, this acidified chamber also provides energy potential for Ca^{2+} to enter lysosomes by H^+/Ca^{2+} exchange, which makes it possible for this organelle functioning as an intracellular Ca^{2+} store. In this regard, several studies have demonstrated that lysosomes act as an important Ca^{2+} store and participate in the physiological regulation of cell functions or activities in a variety of tissues[7-9, 11]. Although the ER may also act as an NAADP–sensitive Ca^{2+} store in some mammalian cells, as mentioned above, a growing body of evidence supports the view that NAADP may mobilize Ca^{2+} from lysosome-related acidic organelles[8, 9, 11, 12]. So far, the precise mechanisms responsible for this NAADP-induced lysosomal Ca^{2+} release remain unknown.

One of possible mechanisms mediating lysosomal Ca^{2+} release is through the ion channel activity of transient receptor potential-mucolipin 1 (TRP-ML1), which is highly expressed and resides in the late endosomes/lysosomes of fibroblast cells[13]. Mutations of TRP-ML1 are implicated in the pathogenesis of a neurological disease, namely, mucolipidosis Type IV (MLIV). MLIV is a neurodegenerative lysosomal storage disease, which appears as psychomotor retardation and visual impairment. The generation of lysosomes from late endosome/lysosome hybrids and lysosomal trafficking within the cells are largely Ca^{2+} - dependent, and a lysosomal TRP-ML1 Ca^{2+} channel may play a key role in Ca^{2+} release from endosome/lysosome vesicles, which trigger the fusion and trafficking of these organelles. The MLIV is genetically attributed to the

mutations in the genes MCOLN1 that encodes the protein TRP-ML1[14, 15]. TRP-ML1 was reported to have a strong topological homology with the polycystin-2 channel[16], and expression of the full-length TRP-ML1 cDNA in *Xenopus* oocytes is associated with the presence of large-conductance channels with permeability to Na^+, K^+, and Ca^{2+} [17] . This TRP protein is also reported to involve agonist-mediated Ca^{2+} signaling in the ER and lysosomes/endosomes, which is dependent on significant permeability to Ca^{2+}[18, 19]. However, many of these studies were done in different cell lines that either lack TRP-ML1 or genetically engineered with TRP-ML1 gene. Little is known whether these TRP subfamily proteins highly expressed in lysosomes possesses channel activity in any native cells and whether this lysosomal TRP member is capable of conducting ion channel activity in CAMs. In a recent study, we provided some preliminary results showing that TRP-ML1 was primarily expressed in lysosomes of native liver cells and an anti-TRP-ML1 antibody could block the NAADP-induced Ca^{2+} conductance of a lipid bilayer reconstituted with liver lysosome proteins[11]. However, the functional relevance and regulation of this lysosomal TRP-ML1 channel activity have yet to be determined in various cell types such as CAMs.

In the present study, we first determined the presence of TRP-ML1 in the lysosomes of CAMs. Second, we analyzed the functional relationship of lysosomal NAADP-sensitive Ca^{2+} channels with TRP-ML1. Then, using isolated and purified lysosomes from coronary arterial smooth muscle we reconstituted the lysosomal NAADP-sensitive Ca^{2+} release channels into a planar lipid bilayer and investigated the characteristics of these channels associated with TRP-ML1. All these experiments attempted to demonstrate TRP-ML1 as a lysosomal NAADP-sensitive Ca^{2+} release channel that exerts critical action in mediation of NAADP-induced increases in intracellular Ca^{2+} levels.

MATERIALS AND METHODS

Culture of CAMs. The bovine CAMs were cultured as described previously[20, 21]. Briefly, the vessels were first rinsed with 5% FBS in medium 199 containing 25 mM HEPES with 1% penicillin, 0.3% gentamycin, and 0.3% nystatin and then cut into segments, and the lumen was filled with 0.4% collagenase in medium 199. After 30 min of incubation at 37°C, the vessels were flushed with medium 199. The strips of denuded arteries were placed into gelatin-coated flasks with medium 199 containing 10% FBS with 1% L-glutamine, 0.1% tylosin, and 1% penicillin-streptomycin. CAMs migrated to the flasks within 3–5 days. Once growth was established, the vessels were removed and cells were grown in medium 199 containing 20% FBS. The identification of CAMs was based on positive staining by an anti-β-actin antibody. All studies were performed with cells of 2 – 4 passages except where specified.

Demonstration of TRP-ML1 expression in coronary arterial myocytes (CAMs): For reverse transcriptase PCR (RT-PCR) analysis, total RNA was isolated from primary cultured CAMs by Trizole (invitrogen, CA, USA), and 25, 50, 100, and 200 ng of different amount of total RNA was transcribed to cDNA by iScripTM cDNA synthesis kit (Invitrogen, CA, USA) in 20 μL reaction mixture. These synthesized cDNAs were used for TRP-ML1 (Accession number: BC118374) PCR reaction by PCR Supermix (Invitrogen, CA, USA) with primers of 5'-GCCAGTTACAGGAACCTCACG-3' and 5'-CCAGAAGGATGTACCAGCCATT-3' at a final concentration of 200 nM. Thirty cycles of PCR were performed in a thermal cycler with a denaturing phase of 30 sec. at 94°C, annealing phase of 45 sec. at 58°C and extension phase of 1 min at 72°C. Glyceraldehyde-3-phosphate dehydrogenase (GAPDH) (Accession number: NM 001034034) was used as control with primers of 5'-CCACGAGAAGTATAACAACACCC-3'

and 5'- TGAAGTCGCAGGAGACAACC-3'. Meanwhile, the levels of TRP-ML subfamily were also determined with primers of 5'-GTTTCATCGGCTAAGGAACT-3' and 5'-TGCCACTGTGAGCTTTATTG-3' for TRP-ML2 (Accession number: XM_611818), and 5'-AATCCTGAGGCTGCTATAAGT-3' and 5'-TAGGAAGAGGTGCTTGAATG-3' for TRP-ML3 (Accession number: XM_592179). A negative control was performed to verify the PCR condition, which contained all the components of the PCR except the template DNA. The PCR products were separated by 1.2 % agarose gel for confirmation of product size.

Cell homogenates of 10, 20, 40, and 60 µg from primary cultures of CAMs were used for Western blot analysis with the methods as we described previously[11]. Anti-TRP-ML1 antibody from Abcam (ab28508, Abcam Inc., MA, USA) was used to probe TRP-ML1 protein according to the manufacturer's instructions and β-actin was used as loading control. The existence of two other TRP-ML subfamily members of TRP-ML2 and TRP-ML3 were examined with corresponding antibodies from Sigma. Meanwhile, the presence of TRPC (Canonical Transient Receptor Potential) channels was also determined with anti-TRPC1 and anti-TRPC3/6/7 antibodies (Santa Cruz Biotechnology, Inc.).

Fluorescence Resonance Energy Transfer (FRET) determining the presence of TRP-ML on lysosomes: Subconfluence CAMs were stained with FITC-conjugated anti-Lamp-1 antibody (553793, BD Pharmingen™, NJ) (FITC/Lamp-1), and TRITC-conjugated $F(ab')_2$ (sc-3841, Santa Cruz Biotechnology Inc.,CA) plus TRP-ML1 primary antibody (ab 28508, Abcam Inc., MA) (TRITC/ TRP-ML1) with a method as described previously[22, 23] and then visualized under confocal microscope with Excitation/Emission wavelength of 494/518 nm and 555/580 nm for FITC and TRITC, respectively. An acceptor bleaching protocol was employed to measure the

FRET efficiency[22, 23] between FITC/Lamp-1 and TRITC/ TRP-ML1, which was calculated through the following formula: $E = (FITCpost - FITCpre)/FITCpost \times 100\%$[22]. TRITC-CTXB (TRITC conjugated with Cholera Toxin subunit B) was paired with FITC-Lamp-1 to act as negative control, since TRITC-CTXB selectively reactes with ganglioside and is widely used for detection of the cell plasma membrane.

RNA interference of TRP-ML1 in CAMs: RNA silence was achieved by double-stranded siRNA of targeting TRP-ML1 (Accession number: BC118374) consisted of 5'-CAGCUUCCGGCUCCUG-3'. A scrambled RNA or Xeragon library scrambled RNA was synthesized for negative control. siRNA transfection was performed according to the manufacturer's instruction in Qiagen TransMessenger kit as we described previously[24]. The final concentration of siRNA was 15 nM and the efficiency of TRP-ML1 silencing was assessed by Western blotting analysis. At 36 h post-transfection, the TRP-ML1-knocked down CAMs were used to measure intracellular Ca^{2+} levels by fluorescent assay or to isolate lysosomes for the channel reconstitution study.

Fluorescent microscopic measurement of $[Ca^{2+}]_i$ in CAMs: Normal CAMs or TRP-ML1 siRNA-treated CAMs were loaded with 10 μM fura-2 at room temperature for 30 min and washed three times with Ca^{2+}-free Hanks' buffer, which was supplemented with 2 μM EGTA. Endothelin-1 (ET-1, 100nM)-induced Ca^{2+} release was performed with a method described previously[9]. A fluorescence ratio of excitation at 340 nm to that at 380 nm (F340/F380) was determined after background subtraction, and $[Ca^{2+}]_i$ was calculated by using the following equation: $[Ca^{2+}]_i = K_d\beta[(R- R_{min})/(R_{max}- R)]$, where K_d for the fura-2-Ca^{2+} complex is 224 nM; R is the fluorescence ratio (F340/F380); R_{max} and R_{min} are the maximal and minimal fluorescence

ratios measured by addition of 10 μM of Ca^{2+} ionophore of ionomycin to Ca^{2+}-replete solution (2.5 mM $CaCl_2$) and Ca^{2+}-free solution (5 mM EGTA), respectively; and β is the fluorescence ratio at 380-nm excitation determined at R_{min} and R_{max}, respectively. Before and after a 100 nM endothelin–1 (ET-1) treatment, the ratio of fura-2 emissions, when excited at the wavelengths of 340 and 380 nm, was recorded with a digital camera (Nikon Diaphoto TMD Inverted Microscope). Metafluor imaging and analysis software was used to acquire, digitize, and store the images for off-line processing and statistical analysis.

Preparation of lysosomes from bovine coronary arterial muscle: CAMs were dissociated from circumflex and left anterior descending arteries of bovine hearts, and CAMs homogenates subsequently were processed to lysosomal isolation and purification with our published methods[11, 25, 26]. The purified lysosomal fraction was suspended in sucrose buffer (0.9% NaCl, 0.3 M sucrose, and 0.1 μM phenylmethylsulfonyl fluoride) and biochemically confirmed[11]. Plasma membrane and SR components were also prepared from bovine coronary arteries as described previously[20, 26], and used as controls. The purity of the lysosomal preparation was biochemically identified[11] and further determined by Western blot analysis using an antibody of LAMP 1 (lysosome-associated membrane protein 1), a lysosomal specific marker, as described previously[11]. The existence of TRP-ML1 and other two TRP-ML subfamily member of TRP-ML2 and TRP-ML3 were also examined. To clarify whether L-type Ca^{2+} channel was expressed on the lysosome, the 1,4-dihydropyridine (DHP) receptor alpha-1 subunit was probed. During Western blot assay, the concentrations of antibodies used were according to the manufacturer's instructions. LAMP1, TRP-ML1 and DHPR alpha 1 antibodies were purchased from Abcam. TRP-ML2, and 3 antibodies were obtained from Sigma and caveolin antibody was purchased from BD Transduction Laboratories, respectively.

Characterization and identity of lysosomal Ca^{2+} release channels: Purified lysosomes were reconstituted into planar lipid bilayers and biophysical characterization of lysosomal Ca^{2+} release channels was performed with a method as we described previously[11, 27, 28]. Pharmacologically, we first investigated the concentration-dependent effects of NAADP on the activity of reconstituted lysosomal Ca^{2+} release channels and then examined the effects of a TRP-ML1 blocker, amiloride (1 mM)[11], an NAADP antagonist of PPADS (50 μM)[29], a common inhibitor of lysosome function of bafilomycin A1 (100 nM), and voltage-dependent Ca^{2+} channel blockers of nifedipine (100 μM) and verapamil (100 μM) on the NAADP-sensitive Ca^{2+} release channel activity[9, 11, 29, 30]. Second, we compared this lysosomal NAADP-sensitive Ca^{2+} release channel with IP_3R and ryanodine receptor/Ca^{2+} (RyR/Ca^{2+}) release channels on the SR by applying IP_3R or RyR agonists and antagonists. Third, we used lysosomes from TRP-ML1 siRNA-treated CAMs or applied immunoprecipitation to deprive TRP-ML1 from the lysosomes to determine whether the channel response to NAADP can be altered. TRP-ML1-deprived lysosome preparations were made as follows: 200 μg lysosome protein in 100 μl resuspension solution was incubated with 10 μg rabbit polyclonal anti-TRP-ML1 antibody (ab28508, Abcam Inc., MA) at 4°C overnight; then 20 μg agarose conjugated goat polyclonal secondary antibody to rabbit IgG H&L was added and further incubated at room temperature for another 2 h, followed by centrifugation at 200 g for 1 min to collect supernatant as TRP-ML1 free lysosomal preparations, so that the immunoprecipitation blocked channel activity would be due to the deprivation of the TRP-ML1 from the lysosomal preparation. Normal rabbit serum was used as a substitute of TRP-ML1 antibody for control preparation. Fourth, we used another anti-TRP-ML1 polyclonal antibody (sc-26269, Santa Cruz Biotechnology Inc., CA), which was raised in goat against a peptide mapping at the C terminus of TRP-ML1 of mouse origin, to test

channel blocking effects. A serial diluted anti-TRP-ML1 antibody was added to the bath solution at a final concentration of 1:5000, 1:500, and 1:50 for 5 min, respectively, followed by 1 μM NAADP. Before and after addition of NAADP, the channel currents were recorded at a holding potential of + 40 mV. Normal goat serum (NGS) was used as a substitute for goat polyclonal TRP-ML1 antibody for control experiments.

Statistics: Data are presented as means ± S.E.; the significance of the differences in mean values between multiple groups was examined using an analysis of variance for repeated measures followed by a Duncan's multiple range test. $p<0.05$ was considered statistically significant.

RESULTS

Expression of TRP-ML1 in CAMs: To demonstrate the presence of TRP-ML1 in the CAMs, we first performed RT-PCR and Western blot analysis to detect TRP-ML1 in CAMs. In Figure 1A, the upper panel presented a typical gel document of RT-PCR products of TRP-ML1 and GAPDH with expected size of 430 and 452bp respectively. The summarized results in the lower panel showed normalized intensity ratio of TRP-ML1 to GAPDH, and no significant ratio differences among the different total RNA groups were observed, which indicated that the amount of TRP-ML1 RT-PCR production was proportional to added total RNA quantity. Similarly, in panel B, Western blot film document and the summarized intensity ratio of TRP-ML1/β-Actin showed that the intensity of individual TRP-ML1 band was proportional to the different amounts of CAMs homogenates loaded. These results provided evidence that the TRP-ML1 gene was expressed in bovine CAMs. In addition, the expression of TRP-ML3 was found in CAMs but not in the purified lysosomes, however; TRP-ML2 was not detected from both mRNA and protein

levels in CAMs. Similarly, TRPC1 and TRPC3, 6, 7 channel proteins were not detected from the purified lysosome preparation (gel document not shown). These results exclude the cross react possibility of TRP-ML1 antibody with TRP-ML2, 3 or any TRPC channels in the subsequent channel characterization studies.

FRET occurrence between FITC/Lamp-1 and TRITC/TRP-ML1**:** In the upper panel of Figure 2A, the green image showed a labeling of lysosomal marker protein of Lamp-1 (FITC/Lamp-1), and the red image showed a labeling of TRP-ML1 (TRITC/TRP-ML1), while the yellow spots in overlaid images represented a colocalization of Lamp-1 and TRP-ML1. In the middle panel images of Figure 2A, the green fluorescence intensity of FITC/Lamp-1 increased after acceptor of TRITC/TRP-ML1 was bleached, while the red fluorescence intensity of TRITC/TRP-ML1 almost disappeared due to bleaching. Yellow spots on the right image were also undetectable in the overlaid image. The lower panel of Figure 2A showed a subtracted image between the Pre- and Post– acceptor bleaching, the blue color intensity represented increased FITC fluorescence due to FRET, and a calculated FRET efficiency was 21.8 ± 6.3%. However, between the pair of TRITC/CTXB (a cell membrane marker) and FITC/Lamp-1, no yellow spots were observed in the overlaid image (image not shown), and FRET efficiency was only 5.1 ± 1.3%. Summarized results in Figure 2B showed that the FRET efficiency between TRITC/TRP-ML1 and FITC/Lamp1 was significantly higher than that from TRITC/CTXB and FITC/Lamp1 group.

TRP-ML1-associated two-phase Ca^{2+} release response in intact CAMs: To determine the role of lysosomal TRP-ML1 in intracellular Ca^{2+} regulation, fluorescent image analysis was conducted to test the effect of TRP-ML1 siRNA on the Ca^{2+} release in intact CAMs in response to 100 nM ET-1, a well-known stimulator of lysosomal Ca^{2+} release[8, 9]. The silencing efficiency of TRP-ML1 siRNA was assessed by Western blotting analysis, and the results

revealed that the expression of TRP-ML1 was decreased by 73.5 ± 6.8 % compared with control group. As shown in Figure 3A, an early Ca^{2+} release (First phase, at 1 min) occurred primarily in the periphery of cells (red dots in the image), followed by a global increase in intracellular Ca^{2+} (red cytosol) (Second phase, at 3 min) in the control group (top panel). Similar to control cells, a two-phase Ca^{2+} release in response to ET-1 was still observed in the cells transfected with scrambled small RNA (middle panel). However, when CAMs were transfected with TRP-ML1 siRNA, ET-1-induced Ca^{2+} increases in both periphery (local) and whole cytosol (global) of the cell were substantially blocked (bottom panel). Figure 3B shows a digitally converted recording of the fura-2 fluorescence ratio F340/F380 against time for $[Ca^{2+}]_i$. Consistent with fluorescence images shown above, there were two peaks when CAMs were treated with ET-1, with a small peak at 1 min corresponding to a local $[Ca^{2+}]_i$ burst and a big peak around 3 min representing the global $[Ca^{2+}]_i$ increase or release of Ca^{2+} from the SR. Calculated Ca^{2+} concentrations from both phase releases were summarized in Figure 3C. Compared to the cells transfected with scrambled small RNA, this lysosome-associated Ca^{2+} release was significantly inhibited in the TRP-ML1 siRNA pre-treated CAMs by 46.8 ± 12.6 % in the local Ca^{2+} burst and 73.3 ± 14.9 % in the global Ca^{2+} wave.

Purification and identification of lysosomes: To study lysosomal channels and related function, purified lysosomes are essential. In the present study, the purity and identity of prepared lysosomes were determined by measurement of various organellar marker enzyme activities and Western blot analysis of organelle specific proteins. As shown in Figure 4, the conversion rate of 4-nitrophenyl phosphate to 4-nitrophenyl by lysosome marker enzyme acid phosphatase was 56.84 ± 7.65, 2.88 ± 2.97 and 0.079 ± 0.157 nmol/min/mg protein in lysosome (Lyso), cell plasma membrane (PM) and SR preparations, respectively. In contrast, reduction rate of

cytochrome *c* by an E(S)R marker enzyme - NADPH-cytochrome c reductase or conversion of sodium thymidine 5-monophosphate *p*-nitrophenyl ester to *p*-nitrophenyl by PM marker - alkaline phosphodiesterase was almost undetectable in lysosome preparations, but they were predominant in SR or PM preparations, respectively. By Western blot analysis, lysosomal membrane-associated protein-Lamp-1 and TRP-ML1 were primarily detected in lysosome preparations, rather than in SR and PM fractions. In contrast, caveolin-1, a PM marker protein was not found in either lysosome or SR fractions. Furthermore, TRP-ML subfamily member TRP-ML2, 3 or dihydropyridine (DHP) receptor alpha-1 subunit was not detected in the lysosomal preparations (Data not shown). These results confirmed that isolated lysosomes from CAMs in the present study are highly purified and free of SR and cell membrane contamination and the identity of lysosomal NAADP-sensitive Ca^{2+} channel may be primarily related with TRP-ML1 protein but not TRP-ML2, 3 or dihydropyridine- sensitive (L-type) Ca^{2+} channels.

I-V relationship and NAADP activation of lysosomal Ca^{2+} release channels: With symmetrical 300 mM cesium in the *cis* and *trans* solution, a unitary Cs^{+} current through reconstituted lysosomal Ca^{2+} channels in the lipid bilayer was recorded at holding potentials from - 40 to + 40 mV (upper panel of Figure 5A). The bottom panel in Figure 5A showed the relationship of holding potentials and channel current amplitudes. Mean slope conductance for these reconstituted SR Cs^{+} currents was 145 ± 35.3 pS with a reversal potential of ~0 mV. Using Ca^{2+} as a carrier charge, we also recorded similar currents, but the channel stability was very low which could not allow us to perform any experiments more than 3 min for characterization. This substitution of Cs^{+} for Ca^{2+} as a charge carrier was widely used for reconstitution of Ca^{2+} channels and in studies on their pharmacological characteristics and physiological regulation of intracellular organelle channels[31, 32].

The concentration-dependent effects of NAADP on the reconstituted lysosomal Ca^{2+} release channel activity were determined. The upper panel of Figure 5B depicts representative recordings of single-channel Cs^{+} currents before and after addition of different doses of NAADP into the *cis* solution under the holding potential of + 40 mV. Summarized results in the bottom panel of Figure 5B showed that the NPo of these channels increased from 0.00925 ± 0.00237 of the control to 0.02 ± 0.00618, 0.0519 ± 0.016 and 0.1287 ± 0.0161 when 10, 100 and 1000 nM of NAADP was added to the *cis* solution, respectively. However, when NAADP concentrations further increased to 10 μM, the channel open probability was reduced to 0.0677 ± 0.0184. Pretreatment of the bilayer with subthreshold NAADP (0.5 nM) also attenuated the effect of a subsequent high dose of NAADP (1 μM) on the channel activity. However, when NAADP was added into the *trans* solution, the channel activation or inhibition was not observed (data not shown), suggesting that NAADP acts on the *cis* side of lysosomes, which corresponds to the cytosolic side.

Effects of IP_3R and RyR agonists and antagonists on lysosomal NAADP-sensitive Ca^{2+} channel activity: Figure 6A depicts representative channel recordings in response to IP_3R and RyR/Ca^{2+} agonists, namely 1 μ IP_3 and 5 μM Rya or their antagonists including 100 μM 2-APB and 50 μM Rya followed by 100 nM NAADP stimulation. In Figure 6B, summarized results showed that the NPo of these channels was 0.00631 ± 0.00251 in the presence of a low concentration of Rya (5 μM), which was not significantly different from 0.00874 ± 0.00361 of control. Rya at this concentration has been reported to significantly activate the RyR/Ca^{2+} release channels on the SR preparations[9, 27]. Moreover, when reconstituted channels were stimulated by 1 μM of IP_3, the NPo of these channels was 0.00635 ± 0.00233, which was also similar to the control. Furthermore, pretreated with a high dose of Rya (50 μM) (inhibitor of RyR/Ca^{2+} release

channels) or 2-APB (100 μM) as the antagonist of IP_3R, it had no significant inhibitory effects on NAADP-induced increase in the NPo of these reconstituted lysosomal Ca^{2+} channels. These results suggest that NAADP-activated lysosomal Ca^{2+} release channels are distinct from the Ins(1,4,5)P_3- and cADPR-sensitive Ca^{2+} stores and corresponding Ca^{2+} release channels on the SR, which are consistent with many reports obtained from measurements of Ca^{2+} release in intact cell preparations such as sea urchin eggs, pancreatic acinar cells, smooth muscle cells and rat liver hepatocytes[9, 11, 33, 34].

Identity of NAADP-sensitive Ca^{2+} release channels: In Figure 7A, summarized results show that NAADP-induced increase in the NP_O of reconstituted lysosomal Ca^{2+} release channels was partially attenuated by amiloride (1 mM), PPADS (50 μM), nifedipine (100 μM), and verapamil (100 μM), but not by bafilomycin A1 (100 nM). The NAADP-induced increase in the NP_O of these Ca^{2+} channels was significantly reduced by 71.5 ± 18.5 % when the cells were treated with the TRP-ML1 siRNA. Similarly, immunoprecipitation or blockade of TRP-ML1 by anti-TRP-ML1 antibodies, the NAADP-induced activation of lysosomal Ca^{2+} channels in bilayer was almost abolished (14.0 ± 4.4 % of NAADP alone group).

Using a TRP-ML1 polyclonal antibody against its C terminus, where the Ca^{2+} channel pore region was located, we further tested whether NAADP-induced activation of these reconstituted lysosomal channels is associated with TRP-ML1. Summarized results in Figure 7B depict that this anti-TRP-ML1 antibody could dose-dependently attenuate NAADP-sensitive lysosomal Ca^{2+} release channel activity. The channel open probability was significantly decreased from 0.1268 ± 0.0213 of control in response to 1 μM NAADP, to 0.1042 ± 0.0169, 0.0467 ± 0.0105 and 0.0249 ± 0.0115, respectively, when a serial antibody concentrations of 1:5000, 1:500 and 1:50 were

added. However, addition of anti-TRP-ML1 antibody to the *trans* solution had no effect on the NAADP-induced activation of lysosomal Ca^{2+} channels (data not shown).

DISCUSSION

In the present study, we used different cells and molecular approaches to show the presence of TRP-ML1-mediated ion channel activity in lysosomes of CAMs and addressed its function as a target protein of NAADP, a potent Ca^{2+} release second messenger in various mammalian cells.

The determination of functional relevance of this lysosomal TRP-ML1 channel protein was based on previous studies that ET-1-induced two-phase Ca^{2+} release is an important functional activity with NAADP as a potent Ca^{2+} release second messenger[8, 9]. The time-course of Ca^{2+} response to ET-1 in coronary arterial myocytes demonstrated two-phase Ca^{2+} release response in our imaging studies, and the corresponding maximal Ca^{2+} responses appeared with a 2 min delay. The time frame (~1 min) of the first phase Ca^{2+} response is very similar to some reports regarding agonist-induced Ca^{2+} release[35, 36]. However, the time lapse that occurred in the second Ca^{2+} release phase after ET-1 stimulation represents a specific feature of NAADP-mediated Ca^{2+} signaling pathway. This time lapse was observed in several previous studies[8, 9]. Although some considered that this two phases Ca^{2+} releasing response is related to Ca^{2+}-induced Ca^{2+} release (CICR), it may represent a special CICR, which is different from the conventional CICR that occurs within seconds rather than minutes. However, the mechanism underlying this NAADP and lysosome-associated CICR with a large time interval is not clear. One possibility is that the global Ca^{2+} release following lysosomal TRP-ML activation or triggering Ca^{2+} release may be associated with lysosomal trafficking to the SR. It seems that small amounts of Ca^{2+}

released from lysosomes may not be enough to activate global Ca^{2+} release from the SR, but are able to drive lysosome movement or aggregation. When these clustered or aggregated lysosomes work together, global Ca^{2+} release is activated. This hypothesis remains to be tested.

Our studies showed efficient silencing of TRP-ML1 gene substantially attenuated local Ca^{2+} burst from lysosomes and subsequent global Ca^{2+} wave by ET-1. These results are very similar to that obtained in studies using pharmacological interventions of lysosome functions such as bafilomycin A1, a lysosomal H^+-ATPase inhibitor, or Gly-Phe-β-naphtylamide (GPN), a lysosomal disruptor[8, 9]. It seems that dependence of the NAADP action on lysosomes is associated with the normal expression and function of TRP-ML1.

During the reconstituting lipid bilayer process, the planar lipid bilayer was formed by painting the mixture of phosphatidylethanolamine and phosphatidylserine (1:1) across a micron-sized aperture in a Delrin Cuvette. The stability of the formed planar lipid bilayer is dependent on the factors of lipid unsaturation degree and headgroup charge, pH, temperature and the presence of cations. Among these factors, the negative charged phosphatidylserine tended to stabilize the bilayer structure. However, when Ca^{2+} was used as the current carrier in the reconstituted bilayer system, it can neutralize the negative charge of phosphatidylserine on the lipid and thereby destablize the bilayer structure[37]. Therefore, Cs^+ has been widely used to substitute Ca^{2+} in the reconstitution of Ca^{2+} channel studies. In native cells, the membrane structure is more complicated and various stabilizing mechanisms of membrane and channels exist in cellular microenvironment. Therefore, Ca^{2+} channel activity using Ca^{2+} carrier charge should be functioning. Although reconstitution studies may not completely replicate the microenvironment

for the channels, studies in this preparation are valuable to define the property of this channel protein. However, the results should be interpreted with caution.

Interestingly, this reconstituted lysosomal channel from coronary arteries was activated by NAADP in a concentration-dependent manner, which was featured by a self-desensitization at high concentrations of NAADP. In addition, pretreatment of the reconstituted bilayer with a subthreshold concentration of NAADP also substantially attenuated NAADP-induced activation of this lysosomal Ca^{2+} channel at successive high concentrations. This self-desensitization property of ion channels has been widely used as a diagnostic tool to confirm the actions of NAADP as Ca^{2+} releasing second messenger[11, 38, 39]. To our knowledge, the functional significance of NAADP desensitization of the lysosomal Ca^{2+} channels remains unknown. Some reports indicated that this self-inactivation might establish subcellular Ca^{2+} memory and control spatiotemporal Ca^{2+} signaling, which is important in the one-time events such as egg fertilization or lymphocyte activation[40, 41]. Pharmacologically, L-type Ca^{2+} channel blockers of nifedipine and verpamil had shown partial inhibitive effects on the NAADP-induced Ca^{2+} channel activity, and these results are consistent with previous studies[11, 30]. However, it should be noted that although L-type Ca^{2+} channel blockers, such as nifedipine, verpamil and diltazen are usually used to pharmacologically characterize NAADP-sensitive Ca^{2+} release channels[1], this inhibitory action of lysosomal channels by L-type Ca^{2+} channel blockers means that these channels may have binding domain for such blockers, but does not mean these channels are L-type Ca^{2+} channels. In facts, NAADP-sensitive Ca^{2+} release channel is a non-selective Ca^{2+} release channel[11, 30]. In addition, the present reconstituted lysosomal channels were blocked by commonly used antagonists of TRP-ML1 channels such as sodium channel antagonist,

amiloride[1] and a NAADP receptor antagonist, PPADS[29], suggesting that the reconstituted lysosomal channel activity is associated with TRP-ML1 function and serves as a target of NAADP action to induce Ca^{2+} release from lysosomes. Nevertheless, bafilomycin A1, a common inhibitor of lysosome function, had no effect on the activity of reconstituted NAADP-sensitive Ca^{2+} release channels. This is not consistent with the observations in intact cells such as pancreatic acinar cells[10], and arterial myocytes[8, 11]. In intact cells, bafilomycin A1 inhibits V-H -ATPase and leads to the depletion of Ca^{2+} storage in their lysosomes. With Ca^{2+} depletion from lysosomes, NAADP-induced Ca^{2+} triggering release and late robust mobilization of Ca^{2+} from the SR/ER are subsequently blocked. However, in the reconstituted system with purified lysosomes used in the present study, only partial lysosome membrane rather than the whole lysosome was incorporated into the lipid bilayer, and therefore there is no Ca^{2+} store or depletion issue in this preparation. Although under this condition bafilomycin A1 may still have an effect on V-H ATPase activity, there is no effect on Ca^{2+} store for channel activity.

Our reconstituted lipid bilayer results also demonstrated that NAADP activated lysosomal Ca^{2+} release channel from the *cis* side rather than the *trans* side, which indicates that the regulatory site of NAADP is only on one side of the channel protein. Given the general agreement that the *cis* side represents the cytosolic side of reconstituted channel proteins[42], it is likely that NAADP acts to the cytosolic side of TRP-ML1 channel in our preparations. These results are consistent with those of previous Ca^{2+} fluorescence measurements in intact cells with microinjection delivering NAADP[43]. Under this situation, NAADP can only bind to the cytosolic side of TRP-ML1, since NAADP is a macromolecule that is impermeable to the lipid-based lysosomal membrane.

Our results that TRP-ML1 may function as the NAADP-sensitive Ca^{2+} release channel are consistent with the properties of classical TRP-ML channels that mediate Ca^{2+}, Na^{+} and K^{+} conductance[44, 45]. In this regard, Some studies showed that TRP-ML1 was a lysosomal monovalent cation channel which may conduct H^{+}[46]. However, those studies were done with cell lines or transgenic cells, where TRP-ML1 was very overly expressed and spread to other compartments of cells[46]. As mentioned by those authors themselves, although the majority of TRP-ML1 is expressed in intracellular compartments in those transgenic human fibroblast cell lines, some of the over-expressed TRP-ML1 was targeted to the plasma membrane (PM). But under a moderate over-expression condition, TRP-ML variants were not found at the PM. Saturation of the protein trafficking pathway by marked over-expression forced expression of significant amounts of TRP-ML1 on the PM. Such PM mistargeting was necessary to study TRP-ML1 channel properties using the whole cell patch clamp configuration[46, 47]. It is obvious that TRP-ML1 on the PM may not occur under native cells. Therefore, the results obtained from the PM may not represent the channel property in lysosomes. In our lysosome preparations from native cells, we found the channels may not conduct H^{+} current, at least under experimental conditions used in the present study.

To further confirm that this reconstituted NAADP-activated Ca^{2+} release channel is associated with TRP-ML1 function, we performed more experiments to test whether knocking down TRP-ML1 gene expression or removal of this protein from lysosome preparations abolished its channel activity induced by NAADP. It was found that silencing the expression of TRP-ML1 gene in CAMs with its specific siRNA substantially attenuated reconstituted lysosomal NAADP-

sensitive Ca^{2+} release channel activity. Similarly, immunoprecipitation of TRP-ML1 from lysosome preparations of CAMS with a specific antibody that was raised against its 101-150th amino acids almost completely abolished the NAADP-related channel activity. Furthermore, another anti-TRP-ML1 antibody mapped at the C terminus of TRP-ML1, a channel pore forming region, was found to dose-dependently attenuate NAADP-induced activation of reconstituted lysosomal Ca^{2+} channels. All these findings from both gene silencing and deprivation of TRP-ML1 protein or interference of its channel pore provide convincing evidence that the activity of this reconstituted lysosomal NAADP-sensitive Ca^{2+} release channel represents a function of TRP-ML1 in CAMs.

In summary, the present study demonstrated that TRP-ML1 was expressed in CAMs and predominantly localized on lysosomes of these cells. This lysosomal protein may function as an NAADP-sensitive Ca^{2+} release channel, which may importantly contribute to ET-1-induced two-phase Ca^{2+} release via NAADP signaling pathway in these arterial myocytes. To our knowledge, these findings provide the first evidence indicating that TRP-ML1 serves as a critical target for the action of NAADP in mediating lysosomal Ca^{2+} release through its channel activity in CAMs. This lysosomal TRP-ML1 channel importantly participates in the Ca^{2+} release response of these cells to some agonists such as ET-1.

SOURCES OF FUNDING

This study was supported by grants from the National Institute of Health (HL-57244, HL-75316, and DK54927).

REFERENCES

1. **Lee HC.** Physiological functions of cyclic ADP-ribose and NAADP as calcium messengers. *Annu Rev Pharmacol Toxicol.* 2001; 41: 317-45.

2. **Bezin S, Charpentier G, Fossier P, Cancela JM.** The Ca^{2+}-releasing messenger NAADP, a new player in the nervous system. *J Physiol Paris.* 2006; 99: 111-8.

3. **Aarhus R, Graeff RM, Dickey DM, Walseth TF, Lee HC.** ADP-ribosyl cyclase and CD38 catalyze the synthesis of a calcium-mobilizing metabolite from NADP. *J Biol Chem.* 1995; 270: 30327-33.

4. **Yamasaki M, Churchill GC, Galione A.** Calcium signalling by nicotinic acid adenine dinucleotide phosphate (NAADP). *Febs J.* 2005; 272: 4598-606.

5. **Dammermann W,Guse AH.** Functional ryanodine receptor expression is required for NAADP-mediated local Ca^{2+} signaling in T-lymphocytes. *J Biol Chem.* 2005; 280: 21394-9.

6. **Gerasimenko JV, Maruyama Y, Yano K, Dolman NJ, Tepikin AV, Petersen OH, Gerasimenko OV.** NAADP mobilizes Ca^{2+} from a thapsigargin-sensitive store in the nuclear envelope by activating ryanodine receptors. *J Cell Biol.* 2003; 163: 271-82.

7. **Churchill GC, Okada Y, Thomas JM, Genazzani AA, Patel S, Galione A.** NAADP mobilizes Ca^{2+} from reserve granules, lysosome-related organelles, in sea urchin eggs. *Cell.* 2002; 111: 703-8.

8. **Kinnear NP, Boittin FX, Thomas JM, Galione A, Evans AM.** Lysosome-sarcoplasmic reticulum junctions. A trigger zone for calcium signaling by nicotinic acid adenine dinucleotide phosphate and endothelin-1. *J Biol Chem.* 2004; 279: 54319-26.

9. **Zhang F, Zhang G, Zhang AY, Koeberl MJ, Wallander E, Li PL.** Production of NAADP and its role in Ca^{2+} mobilization associated with lysosomes in coronary arterial myocytes. *Am J Physiol Heart Circ Physiol.* 2006; 291: H274-82.

10. **Yamasaki M, Masgrau R, Morgan AJ, Churchill GC, Patel S, Ashcroft SJ, Galione A.** Organelle selection determines agonist-specific Ca^{2+} signals in pancreatic acinar and beta cells. *J Biol Chem.* 2004; 279: 7234-40.

11. **Zhang F,Li PL.** Reconstitution and characterization of a nicotinic acid adenine dinucleotide phosphate (NAADP)-sensitive Ca^{2+} release channel from liver lysosomes of rats. *J Biol Chem.* 2007; 282: 25259-69.

12. **Genazzani AA,Galione A.** Nicotinic acid-adenine dinucleotide phosphate mobilizes Ca^{2+} from a thapsigargin-insensitive pool. *Biochem J.* 1996; 315 (Pt 3): 721-5.

13. **Luzio JP, Bright NA, Pryor PR.** The role of calcium and other ions in sorting and delivery in the late endocytic pathway. *Biochem Soc Trans.* 2007; 35: 1088-91.

14. **Bach G.** Mucolipin 1: endocytosis and cation channel--a review. *Pflugers Arch.* 2005; 451: 313-7.

15. **LaPlante JM, Ye CP, Quinn SJ, Goldin E, Brown EM, Slaugenhaupt SA, Vassilev PM.** Functional links between mucolipin-1 and Ca^{2+}-dependent membrane trafficking in mucolipidosis IV. *Biochem Biophys Res Commun.* 2004; 322: 1384-91.

16. **Sun M, Goldin E, Stahl S, Falardeau JL, Kennedy JC, Acierno JS, Jr., Bove C, Kaneski CR, Nagle J, Bromley MC, Colman M, Schiffmann R, Slaugenhaupt SA.** Mucolipidosis type IV is caused by mutations in a gene encoding a novel transient receptor potential channel. *Hum Mol Genet.* 2000; 9: 2471-8.

17. **Cantiello HF, Montalbetti N, Goldmann WH, Raychowdhury MK, Gonzalez-Perrett S, Timpanaro GA, Chasan B.** Cation channel activity of mucolipin-1: the effect of calcium. *Pflugers Arch.* 2005; 451: 304-12.

18. **Harhun M, Gordienko D, Kryshtal D, Pucovsky V, Bolton T.** Role of intracellular stores in the regulation of rhythmical $[Ca^{2+}]_i$ changes in interstitial cells of Cajal from rabbit portal vein. *Cell Calcium.* 2006; 40: 287-98.

19. **Vanden Abeele F, Lemonnier L, Thebault S, Lepage G, Parys JB, Shuba Y, Skryma R, Prevarskaya N.** Two types of store-operated Ca^{2+} channels with different activation modes and molecular origin in LNCaP human prostate cancer epithelial cells. *J Biol Chem.* 2004; 279: 30326-37.

20. **Li PL, Chen CL, Bortell R, Campbell WB.** 11,12-Epoxyeicosatrienoic acid stimulates endogenous mono-ADP-ribosylation in bovine coronary arterial smooth muscle. *Circ Res.* 1999; 85: 349-56.

21. **Li PL, Zou AP, Campbell WB.** Regulation of KCa-channel activity by cyclic ADP-ribose and ADP-ribose in coronary arterial smooth muscle. *Am J Physiol.* 1998; 275: H1002-10.

22. **Nieminen J, Kuno A, Hirabayashi J, Sato S.** Visualization of galectin-3 oligomerization on the surface of neutrophils and endothelial cells using fluorescence resonance energy transfer. *J Biol Chem.* 2007; 282: 1374-83.

23. **Kenworthy AK, Petranova N, Edidin M.** High-resolution FRET microscopy of cholera toxin B-subunit and GPI-anchored proteins in cell plasma membranes. *Mol Biol Cell.* 2000; 11: 1645-55.

24. **Zhang G, Zhang F, Muh R, Yi F, Chalupsky K, Cai H, Li PL.** Autocrine/paracrine pattern of superoxide production through NAD(P)H oxidase in coronary arterial myocytes. *Am J Physiol Heart Circ Physiol.* 2007; 292: H483-95.

25. **Li PL,Campbell WB.** Epoxyeicosatrienoic acids activate K^+ channels in coronary smooth muscle through a guanine nucleotide binding protein. *Circ Res.* 1997; 80: 877-84.

26. **Yi XY, Li VX, Zhang F, Yi F, Matson DR, Jiang MT, Li PL.** Characteristics and actions of NAD(P)H oxidase on the sarcoplasmic reticulum of coronary artery smooth muscle. *Am J Physiol Heart Circ Physiol.* 2006; 290: H1136-44.

27. **Li PL, Tang WX, Valdivia HH, Zou AP, Campbell WB.** cADP-ribose activates reconstituted ryanodine receptors from coronary arterial smooth muscle. *Am J Physiol Heart Circ Physiol.* 2001; 280: H208-15.

28. **Tang WX, Chen YF, Zou AP, Campbell WB, Li PL.** Role of FKBP12.6 in cADPR-induced activation of reconstituted ryanodine receptors from arterial smooth muscle. *Am J Physiol Heart Circ Physiol.* 2002; 282: H1304-10.

29. **Billington RA,Genazzani AA.** PPADS is a reversible competitive antagonist of the NAADP receptor. *Cell Calcium.* 2007; 41: 505-11.

30. **Yusufi AN, Cheng J, Thompson MA, Burnett JC, Grande JP.** Differential mechanisms of Ca^{2+} release from vascular smooth muscle cell microsomes. *Exp Biol Med (Maywood).* 2002; 227: 36-44.

31. **Anyatonwu GI, Buck ED, Ehrlich BE.** Methanethiosulfonate ethylammonium block of amine currents through the ryanodine receptor reveals single pore architecture. *J Biol Chem.* 2003; 278: 45528-38.

32. **Tinker A, Lindsay AR, Williams AJ.** A model for ionic conduction in the ryanodine receptor channel of sheep cardiac muscle sarcoplasmic reticulum. *J Gen Physiol.* 1992; 100: 495-517.

33. **Churchill GC,Galione A.** Spatial control of Ca^{2+} signaling by nicotinic acid adenine dinucleotide phosphate diffusion and gradients. *J Biol Chem.* 2000; 275: 38687-92.

34. **Cancela JM, Churchill GC, Galione A.** Coordination of agonist-induced Ca^{2+}-signalling patterns by NAADP in pancreatic acinar cells. *Nature.* 1999; 398: 74-6.

35. **Guibert C,Beech DJ.** Positive and negative coupling of the endothelin ETA receptor to Ca^{2+}-permeable channels in rabbit cerebral cortex arterioles. *J Physiol.* 1999; 514 (Pt 3): 843-56.

36. **Barone F, Genazzani AA, Conti A, Churchill GC, Palombi F, Ziparo E, Sorrentino V, Galione A, Filippini A.** A pivotal role for cADPR-mediated Ca^{2+} signaling: regulation of endothelin-induced contraction in peritubular smooth muscle cells. *Faseb J.* 2002; 16: 697-705.

37. **Albert AD, Sen A, Yeagle PL.** The effect of calcium on the bilayer stability of lipids from bovine rod outer segment disk membranes. *Biochim Biophys Acta.* 1984; 771: 28-34.

38. **Aarhus R, Dickey DM, Graeff RM, Gee KR, Walseth TF, Lee HC.** Activation and inactivation of Ca^{2+} release by $NAADP^{+}$. *J Biol Chem.* 1996; 271: 8513-6.

39. **Genazzani AA, Empson RM, Galione A.** Unique inactivation properties of NAADP-sensitive Ca^{2+} release. *J Biol Chem.* 1996; 271: 11599-602.

40. **Churchill GC,Galione A.** Prolonged inactivation of nicotinic acid adenine dinucleotide phosphate-induced Ca^{2+} release mediates a spatiotemporal Ca^{2+} memory. *J Biol Chem.* 2001; 276: 11223-5.

41. **Chini EN,De Toledo FG.** Nicotinic acid adenine dinucleotide phosphate: a new intracellular second messenger? *Am J Physiol Cell Physiol.* 2002; 282: C1191-8.

42. **Zhang DX, Chen YF, Campbell WB, Zou AP, Gross GJ, Li PL.** Characteristics and superoxide-induced activation of reconstituted myocardial mitochondrial ATP-sensitive potassium channels. *Circ Res.* 2001; 89: 1177-83.

43. **Boittin FX, Galione A, Evans AM.** Nicotinic acid adenine dinucleotide phosphate mediates Ca^{2+} signals and contraction in arterial smooth muscle via a two-pool mechanism. *Circ Res.* 2002; 91: 1168-75.

44. **LaPlante JM, Falardeau J, Sun M, Kanazirska M, Brown EM, Slaugenhaupt SA, Vassilev PM.** Identification and characterization of the single channel function of human mucolipin-1 implicated in mucolipidosis type IV, a disorder affecting the lysosomal pathway. *FEBS Lett.* 2002; 532: 183-7.

45. **Raychowdhury MK, Gonzalez-Perrett S, Montalbetti N, Timpanaro GA, Chasan B, Goldmann WH, Stahl S, Cooney A, Goldin E, Cantiello HF.** Molecular pathophysiology of mucolipidosis type IV: pH dysregulation of the mucolipin-1 cation channel. *Hum Mol Genet.* 2004; 13: 617-27.

46. **Kiselyov K, Chen J, Rbaibi Y, Oberdick D, Tjon-Kon-Sang S, Shcheynikov N, Muallem S, Soyombo A.** TRP-ML1 is a lysosomal monovalent cation channel that undergoes proteolytic cleavage. *J Biol Chem.* 2005; 280: 43218-23.

47. **Soyombo AA, Tjon-Kon-Sang S, Rbaibi Y, Bashllari E, Bisceglia J, Muallem S, Kiselyov K.** TRP-ML1 regulates lysosomal pH and acidic lysosomal lipid hydrolytic activity. *J Biol Chem.* 2006; 281: 7294-301.

FIGURE LEGENDS

Figure 1. TRP-ML1 mRNA and protein expression in CAMs. Figure 1A: representative gel document of RT-PCR products of TRP-ML1 and GAPDH at different initial RNA concentrations (upper panel). Summarized results in lower panel shows normalized intensity ratio of TRP-ML1 to GAPDH. Figure 1B: Western blot gel document presents the level of TRP-ML1 and β-actin from CAMs homogenates at different concentrations (upper panel). Summarized results in lower panel shows normalized intensity ratio of TRP-ML1 to β-Actin (n = 5 batches of cell preparations).

Figure 2. FRET detection of FITC-labeled Lamp-1 and TRITC-labeled TRP-ML1 in CAMs. In Figure 2A, the upper panel shows fluorescent images of a FITC/Lamp1 and TRITC/TRP-ML1 before acceptor bleaching (TRITC bleaching). The middle panel shows corresponding fluorescent images after acceptor bleaching. The bottom panel presents fluorescent images obtained by subtraction of post-bleaching images from pre-bleaching images (the middle panel minus the upper panel). Summarized results in Figure 2B showed that the FRET efficiency in TRITC/CTXB control group and TRITC/TRP-ML1 experimental group. * $p<0.05$, significant difference from TRITC/CTXB group (n = 6).

Figure 3. ET-1-induced Ca^{2+} release response in TRP-ML1 siRNA treated CAMs. Panel A: serial images of fura-2 fluorescence ratio F340/F380 recorded in different treated CAMs. Spatially localized Ca^{2+} burst (First phase) around the cell boundary preceded global Ca^{2+} wave

(Second phase) in control and scrambled groups after ET-1 treatment with significantly blocking effects in TRP-ML1-siRNA group. Panel B: an online recording of fura-2 fluorescence ratio of F340 *vs.* F380 (F340/F380) against time. Panel C: Summarized results. * $p < 0.05$ vs. control or scrambled RNA group (n = 6).

Figure 4. Purity confirmation of lysosome preparations. Summarized results shows the conversion rate of 4-nitrophenyl phosphate to 4-nitrophenyl by a lysosome marker enzyme, acid phosphatase in lysosomes (*Lyso*), sarcoplasmic reticulum (*SR*), and plasma membrane (*PM*), the reduction of cytochrome *c* by an E(S)R marker enzyme, NADPH cytochrome *c* reductase in the presence of NADPH, and the conversion rate of sodium thymidine 5'-monophosphate *p*-nitrophenyl ester to *p*-nitrophenyl by a plasma membrane marker enzyme, alkaline phosphodiesterase. * $p<0.05$, significant difference from other groups (n = 6 batches of lysosomal preparations).

Figure 5. Electrophysiological and pharmacological characterization of reconstituted lysosomal Ca^{2+} release channels. A: representative recording of NAADP-sensitive Ca^{2+} channel currents in the upper panel at holding potential of -40 to +40 mV. c: channel closed. *Insert*: scales of channel recording time (50 mS) and amplitude (10 pA). The bottom panel presents a current-voltage relationship of reconstituted lysosomal Ca^{2+} -release channels with symmetrical cesium methanesulfonate (300 mM) solution. B: The upper panel shows representative recordings of reconstituted lysosomal NAADP-sensitive Ca^{2+} release channels in the planar lipid bilayer under control condition or with treatment of NAADP. The bottom panel summarized *NP*o (open channel probability) when CAMs were treated with different concentrations of NAADP. '0.5 nM

then 1 μM' means pretreatment of the bilayer with subthreshold NAADP (0.5 nM) followed by a high dose of NAADP (1 μM). * $p<0.05$, significant difference from control group (n = 6).

Figure 6. Effects of IP_3R or RyR agonist and antagonist on the activity of reconstituted lysosomal Ca^{2+} release channels. A: representative recordings of channel currents under control condition and after addition of NAADP (100nM), IP_3 (1 μM) and Rya (5 μM) or pretreated with 2-APB (100 μM) or Rya (50 μM) followed by NAADP (100 nM) into the *cis* solution. B: summarized channel open probability (NPo) at different treatments. * $p< 0.05$ compared with NAADP alone group (n = 6).

Figure 7. Identification of lysosomal NAADP-sensitive Ca^{2+} release channels as TRP-ML1 function by reconstituted lipid bilayer assay. A: Summarized results shows that the channel open probability (NPo) is under control condition and by treatment of bilayer with 100 nM NAADP before and after pretreatment of amiloride (1 mM), PPADS (50 μM), nifedipine (100 μM), verapamil(100 μM), bafilomycin A1(100 nM) and TRP-ML1 siRNA or immunoprecipitation of TRP-ML1 by anti-TRP-ML1 antibody (ab28508, Abcam). B: Summarized results show that the NAADP-induced channel NPo is under control condition, by treatment of bilayer with normal goat serum (NGS) or after anti-TRP-ML1 antibody (sc-26269, Santa Cruz Biotechnology) addition, respectively. # $p<0.05$ compared to NAADP alone group; * $p< 0.05$ compared to control or NGS-treated group (n = 6).

Figure 1

A

TRP-ML1 — 430bp

GAPDH — 452bp

25 50 100 200

Total RNA (ng)

Normalized intensity ratio (TRP-ML1/GAPDH)

0.0 0.1 0.2 0.3 0.4

25 50 100 200

Total RNA(ng)

B

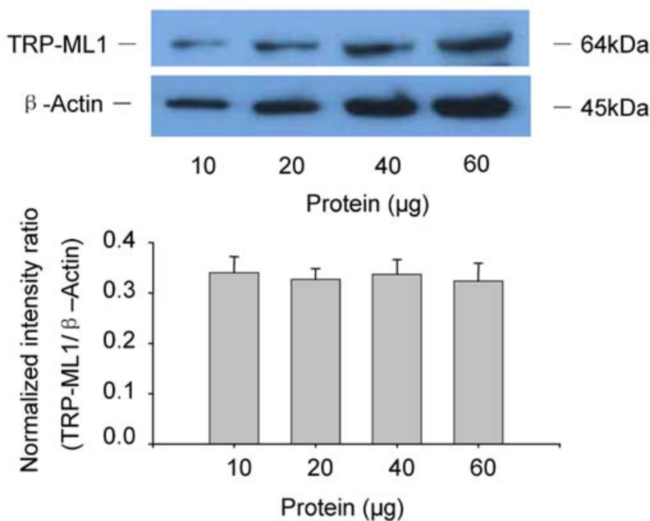

Figure 2

A

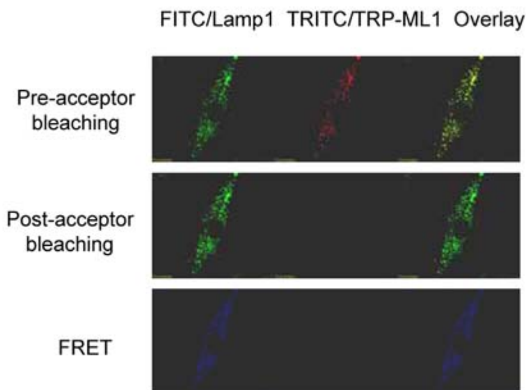

B

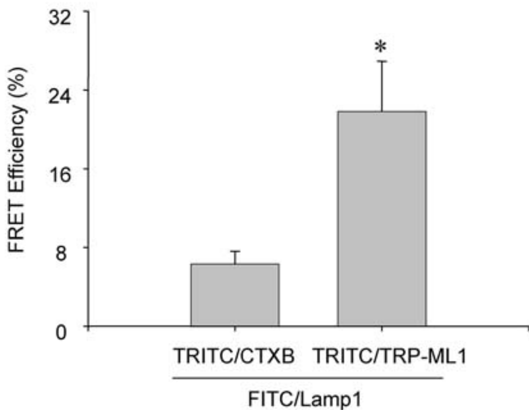

Figure 3

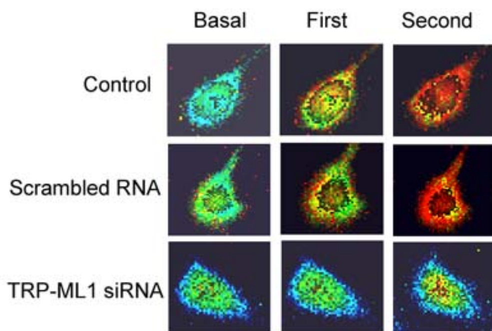

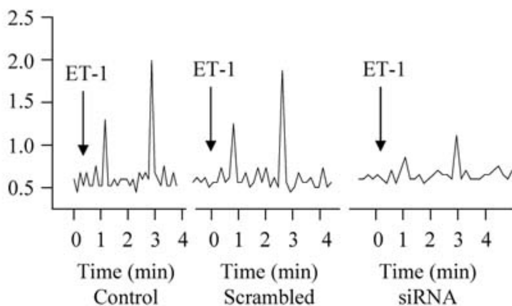

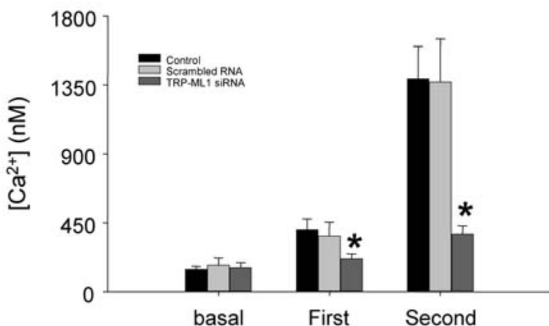

Figure 4

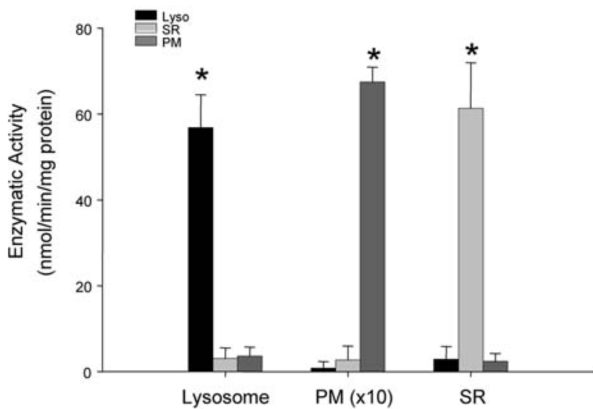

Figure 5A

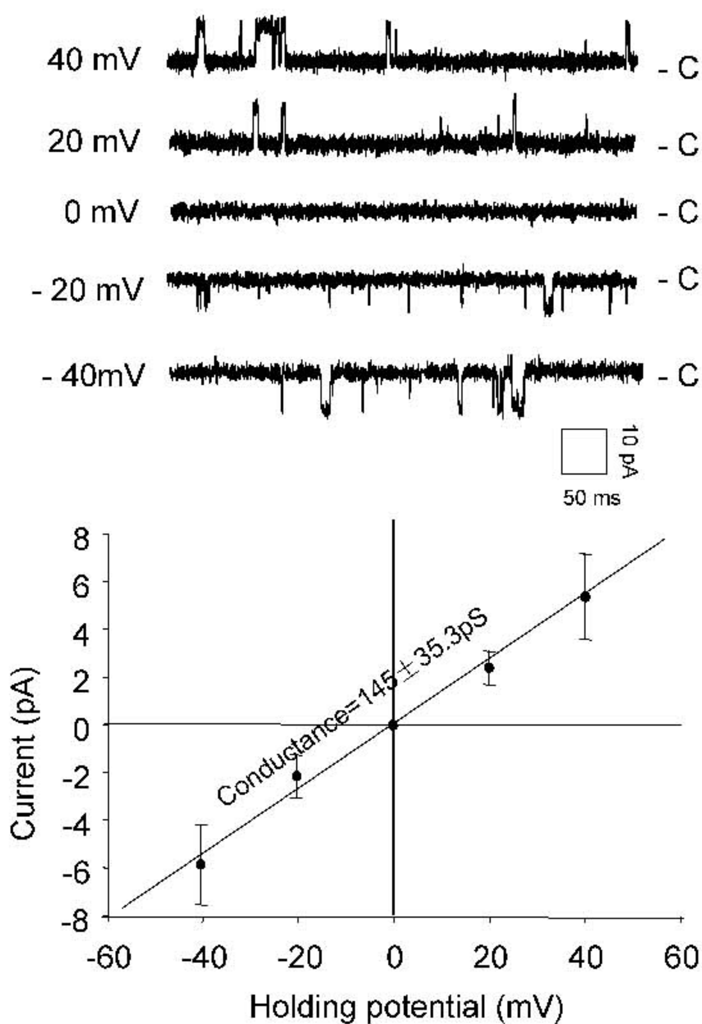

Figure 5B

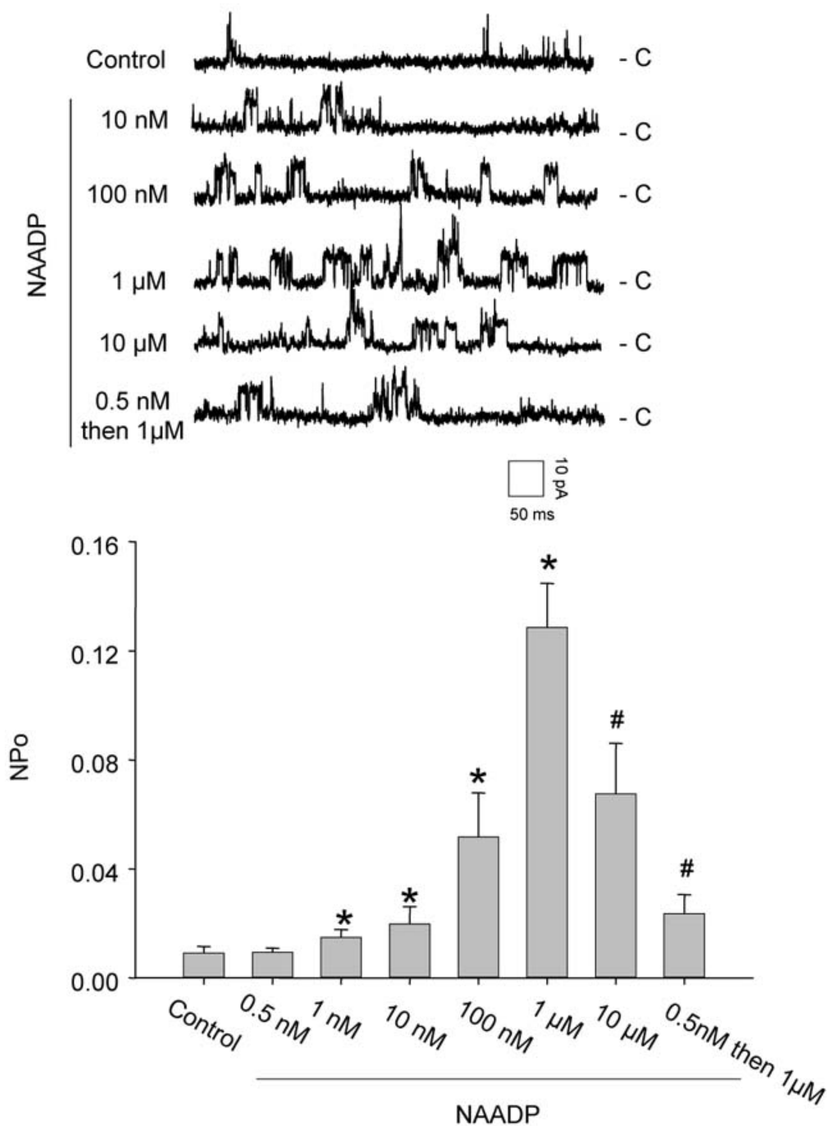

Figure 6

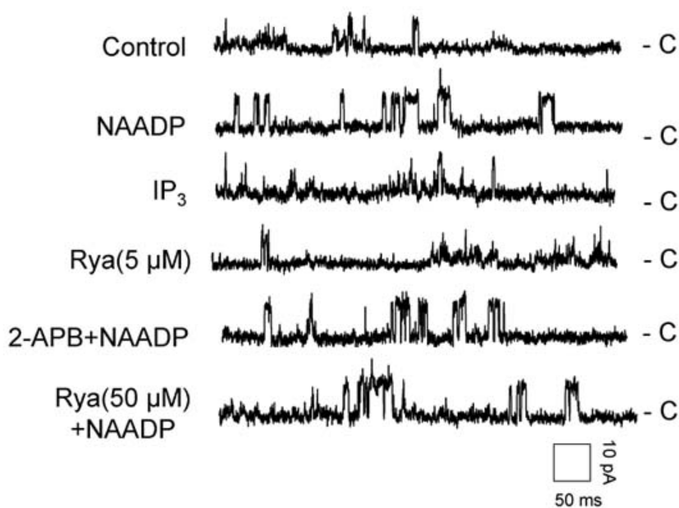

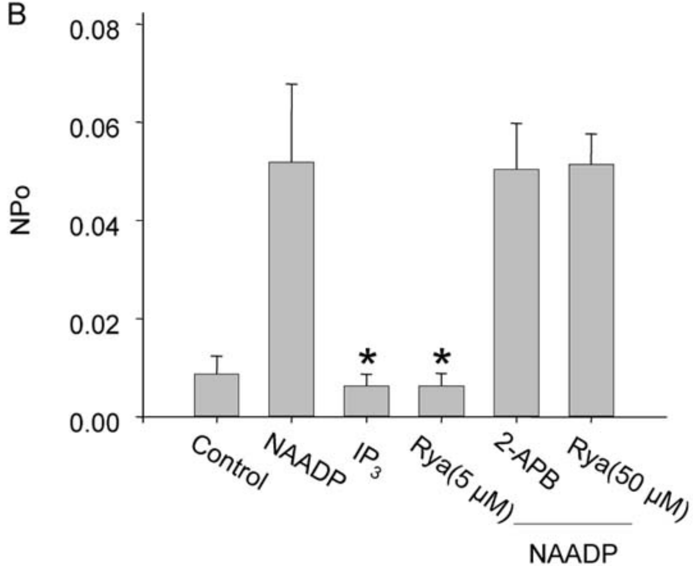

Figure 7

A

0.08
0.06
0.04
0.02
0.00
NPo
#
Control
NAADP
Amiloride
PPADS
Nifedipine
Verapamil
Bafilomycin A1
TRP-ML1 IP
TRP-ML1 siRNA
NAADP